

Pairing symmetry and properties of iron-based high temperature superconductors

Yuan Wan and Qiang-Hua Wang*

National Laboratory of Solid State Microstructures & Department of Physics, Nanjing University, Nanjing 210093, China
(Dated: September 20, 2018)

Pairing symmetry is important to identify the pairing mechanism. The analysis becomes particularly timely and important for the newly discovered iron-based multi-orbital superconductors. From group theory point of view we classified all pairing matrices (in the orbital space) that carry irreducible representations of the system. The quasiparticle gap falls into three categories: full, nodal and gapless. The nodal-gap states show conventional Volovik effect even for on-site pairing. The gapless states are odd in orbital space, have a negative superfluid density and are therefore unstable. In connection to experiments we proposed possible pairing states and implications for the pairing mechanism.

Introduction The newly discovered family of iron-based ReOFeAs (Re = La, Ce, Pr, etc.) high temperature superconductors are raising great interests in the community.[1] The superconductor consists of layers of FeAs which is believed to be the conducting planes. The ReO layers in between the FeAs layers stabilize the structure and donate carriers to the FeAs layers. For example, substitution of O by F or introducing O vacancies[2] dopes electrons into the system, and contrarily substitution of Re by alkaline-earth elements can realize hole doping.[3] Some preliminary experimental results on the superconducting (SC) state have been obtained. The specific capacity measurement[4] and nuclear magnetic resonance (NMR) [5] indicate a nodal gap, and the existence of Andreev bound state implies a non-trivial phase structure of SC gap[6], while both s-wave and dirty d-wave behaviors are suggested by penetrate length measurement[7]. On the theoretical side, local-density-approximation (LDA) calculations show that the states near the Fermi level are largely contributed by the five d-orbitals. [8] Moreover, some authors demonstrated that it is sufficient to keep only a few of them, for example the d_{xz} and d_{yz} orbitals, to reproduce qualitatively the LDA Fermi surface topology.[9] As for the driving force for superconducting pairing, both electronic[10] and phonon-mediated mechanisms[11] are proposed, and various pairing symmetries are predicted.

Since the pairing symmetry is related to the pairing mechanism, a classification of all possible pairing symmetries [12] is important. This is more so given the fact that the pairing function becomes an orbital-wise matrix function in the multi-orbital case, which we elaborate in this paper. The main results are as follows. 1) From a two-orbital ($d_{xz} + d_{yz}$) model we classify all possible on-site and bond-wise pairing basis matrices. In addition to the momentum dependence, the matrices themselves carry nontrivial symmetries, so that even on-site pairing may lead to a nodal or gapless pairing. 2) In the gapless case the density of states (DOS) at the fermi level is enhanced by the SC order. 3) Only the nodal-gap cases show Volovik effect in an applied magnetic field. 4) Most surprisingly, the gapless SC state may have a negative su-

perfluid density, and is therefore unstable against phase twisting. 5) In connection to available experiments we propose possible pairing bases and further experiments to reduce the candidate list.

Symmetry Analysis In the FeAs layer there are two Fe ions per unit cell because of the As ions. In order to simplify the analysis, we adopt a two-band model, i.e. we keep the two atomically degenerate d_{xz} and d_{yz} orbitals of Fe ion, which are important for superconductivity, and neglect d_{xy} , $d_{x^2-y^2}$ and $d_{3z^2-r^2}$ orbitals of Fe ions and all orbitals of As ions for a moment. Thus we will focus on the Fe-lattice, for which there is only one Fe ion in each unit cell. The effect of As ions can be partially included in the effective hopping integrals for the d-orbitals. We define x - and y -direction unitary vectors as connecting the nearest neighbor Fe-atoms. The space group of our model is $P4/mmm$, which has higher symmetry than the space group of whole system $P4/nmm$. The normal state of the model can be described by, in the momentum space, $H_0 = \sum_{k\sigma} \phi_{k\sigma}^\dagger \xi_k \phi_{k\sigma}$ where $\phi_k^\dagger = (d_{xz}^\dagger, d_{yz}^\dagger)_{k\sigma}$, and $\xi_k = \epsilon_k \tau_0 + \delta_k \tau_3 + \gamma_k \tau_1$ in which $\tau_{0,1,3}$ are unit and Pauli matrices defined in the orbital space. For point group operations under concern, the d_{xz} and d_{yz} orbital wave functions transform as x and y , respectively. This dictates that $\phi_k^\dagger \tau_0 \phi_k$ transforms as A_{1g} , $\phi_k^\dagger \tau_1 \phi_k$ as B_{2g} , $\phi_k^\dagger \tau_2 \phi_k$ (which is actually absent in H_0 but is included here for later use) as A_{2g} , and $\phi_k^\dagger \tau_3 \phi_k$ as B_{1g} . Equivalently we claim that the τ -matrices carries the above-mentioned irreducible representations, without referring to the orbital wave functions further. Finally to leave H_0 invariant, ϵ_k , δ_k and γ_k must transform as A_{1g} , B_{1g} and B_{2g} , respectively. The concrete form of the dispersions in H_0 (see below) is irrelevant at this stage.

We now discuss the pairing symmetry. The system is invariant under spin-SU(2) transformation and one can classify the pairing states into spin-singlet and spin-triplet cases, which we assign in the last step according to the global antisymmetry of the pairing function with respect to the combined exchange of spin, orbital and spatial position. We therefore concentrate first on the symmetry of pairing as a function of momentum and a matrix in the orbital space. Since the pairing

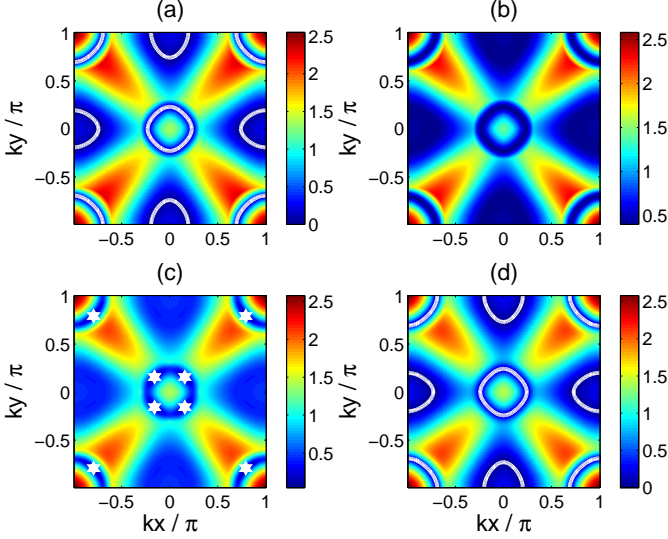


FIG. 1: (Color) Minimal quasiparticle excitation energy as a function of momentum in the normal state (a), a full-gap SC state (b), a nodal-gap SC state (c) and a gapless SC state (d). Thick white lines (symbols) indicate the Fermi surface (nodal points).

operator $\phi_{\alpha\sigma}(-k)\tau_i^{\alpha\beta}\phi_{\beta\sigma'}(k)$ (where $\phi_{\alpha,\beta} = d_{xz,yz}$ and $i = 0, 1, 2, 3$) transforms identically as $\phi_{\alpha\sigma}^\dagger(k)\tau_i^{\alpha\beta}\phi_{\beta\sigma'}(k)$, we immediately see that the τ -matrices in the pairing matrix transform exactly as they do in H_0 . For on-site pairing, $\tau_{0,1,2,3}$ carries the irreducible representations. Since $\tau_{0,1,3}$ are even in orbital space and transform as A_{1g} , B_{2g} and B_{1g} under the point group, the spin channel must be a singlet. On the other hand, $i\tau_2$ is odd in orbital space and transform as A_{2g} , the spin channel must be in a triplet.

The extension to pairing on bonds is almost straightforward. We may multiply the above mentioned τ -matrices by trigonometric basis functions to form the pairing matrices corresponding to pairing on bonds in real space. For the system under concern, the basis functions for nearest-neighbor bonds are $\cos k_x + \cos k_y$ (A_{1g}), $\cos k_x - \cos k_y$ (B_{1g}), $(\sin k_x, \sin k_y)$ (carrying the two-dimensional E_g representation). The symmetry of the product is easily seen from that fact that the τ -matrices only carry one-dimensional representations. For example, $B_{1g} \cdot \tau_1 \sim B_{1g} \cdot B_{2g} \sim A_{2g}$. Since the orbital parity is even, the spin channel must be a singlet. In Tab.I we list all possible pairing basis matrices for on-site pairing and nearest-neighbor-bond pairing (extension to longer-range pairing is trivial), together with the irreducible representations they carry, the spin symmetry, orbital parity, and the behavior of the corresponding quasiparticle excitation gap in the momentum space (which will be discussed later). We notice that even on-site pairing can carry a non-trivial representation, indicating the unique role of the two (atomically) degenerate d-wave orbitals.

TABLE I: Pairing basis matrices carrying irreducible representations of the model. The first column is the index number, the second and the third columns list the representations and the basis matrix functions. The spin and orbital parities are shown in the forth and the fifth columns. The last column describe the behavior of quasiparticle excitation gap in the momentum space. Notice that $\tau_{0,1,2,3}$ transform as $A_{1g}, B_{2g}, A_{2g}, B_{1g}$ respectively due to two xz and yz orbitals. These rules are important to identify the global symmetry and the gap behavior of the basis matrix function.

No.	IR	Basis	Spin	Orbital Parity	Gap
1	A_{1g}	τ_0	S	E	Full
2	A_{1g}	$(\cos k_x + \cos k_y)\tau_0$	S	E	Nodal
3	A_{1g}	$(\cos k_x - \cos k_y)\tau_3$	S	E	Nodal
4	A_{2g}	$(\cos k_x - \cos k_y)\tau_1$	S	E	Nodal
5	B_{1g}	τ_3	S	E	Nodal
6	B_{1g}	$(\cos k_x - \cos k_y)\tau_0$	S	E	Nodal
7	B_{1g}	$(\cos k_x + \cos k_y)\tau_3$	S	E	Nodal
8	B_{2g}	τ_1	S	E	Nodal
9	B_{2g}	$(\cos k_x + \cos k_y)\tau_1$	S	E	Nodal
10	E_g	$\begin{cases} \sin k_x i\tau_2 \\ \sin k_y i\tau_2 \end{cases}$	S	O	Gapless
10'	E_g	$\begin{cases} (\sin k_x + i \sin k_y)i\tau_2 \\ (\sin k_x - i \sin k_y)i\tau_2 \end{cases}$	S	O	Gapless
11	A_{2g}	$i\tau_2$	T	O	Gapless
12	A_{2g}	$(\cos k_x + \cos k_y)i\tau_2$	T	O	Gapless
13	B_{2g}	$(\cos k_x - \cos k_y)i\tau_2$	T	O	Gapless
14	E_g	$\begin{cases} \sin k_x \tau_0 \\ \sin k_y \tau_0 \end{cases}$	T	E	Nodal
14'	E_g	$\begin{cases} (\sin k_x + i \sin k_y)\tau_0 \\ (\sin k_x - i \sin k_y)\tau_0 \end{cases}$	T	E	Full
15	E_g	$\begin{cases} \sin k_x \tau_3 \\ \sin k_y \tau_3 \end{cases}$	T	E	Nodal
15'	E_g	$\begin{cases} (\sin k_x + i \sin k_y)\tau_3 \\ (\sin k_x - i \sin k_y)\tau_3 \end{cases}$	T	E	Nodal
16	E_g	$\begin{cases} \sin k_x \tau_1 \\ \sin k_y \tau_1 \end{cases}$	T	E	Nodal
16'	E_g	$\begin{cases} (\sin k_x + i \sin k_y)\tau_1 \\ (\sin k_x - i \sin k_y)\tau_1 \end{cases}$	T	E	Nodal

Quasiparticle excitation gap To illustrate the concrete gap structure in the various SC states, we need the band structure of iron-based superconductors. Here we adopt the tight-binding model introduced by Ref.[13]. The BdG Hamiltonian is given by $H = \sum_k \psi_k^\dagger H_k \psi_k$, where we recall that the momentum is defined in the "large" Brillouin (BZ) corresponding to one Fe per unit cell, $\psi_k = (d_{xz,k\uparrow}, d_{yz,k\uparrow}, d_{xz,-k\downarrow}^\dagger, d_{yz,-k\downarrow}^\dagger)^T$ is the four-component spinor in the orbital and Nambu space, and

H_k is, in a form of block-matrix,

$$H_k = \begin{pmatrix} \xi_k & V\Delta_k \\ V\Delta_k^\dagger & -\xi_k \end{pmatrix}.$$

Here $\xi_k = \epsilon_k\tau_0 + \delta_k\tau_3 + \gamma_k\tau_1$ is a tight-binding dispersion defined in H_0 , with $\epsilon_k = -(t_1 + t_2)(\cos k_x + \cos k_y) - 4t_3 \cos k_x \cos k_y - \mu$, $\delta_k = -(t_1 - t_2)(\cos k_x - \cos k_y)$, and $\gamma_k = -4t_4 \sin k_x \sin k_y$. Here $t_1 = -1$, $t_2 = -1.3$, $t_3 = t_4 = -0.85$, and $\mu = 1.45$, in unit of $|t_1|$. The gap amplitude $V = 0.4$ is chosen for illustration, and Δ_k is selected from the basis matrix functions listed in Tab.I. The hamiltonian can be exactly diagonalized to obtain the quasiparticle excitations and other SC properties. Zero energy excitations are determined by $\det(H_k) = 0$. In the case of SC state No.1 in Tab.I, $\det(H_k) = (\epsilon_k^2 - \delta_k^2 - \gamma_k^2 - V^2)^2 + (2V\epsilon_k)^2 = 0$ has no solution. This corresponds to the full-gapped case. For SC state No.5, $\det(H_k) = (\epsilon_k^2 - \delta_k^2 - \gamma_k^2 + V^2)^2 + (2V\delta_k)^2 = 0$ is satisfied at four sets of nodal points in BZ. Another interesting example is SC state No.11, for which $\det(H_k) = (\epsilon_k^2 - \delta_k^2 - \gamma_k^2 + V^2)^2 = 0$ holds along lines in BZ. Such zero-lines form the fermi surface (FS) (slightly different from the normal state FS) for the BdG quasiparticles. This is the gapless case.

Due to the two-orbital character of the SC state, the nodal points or the BdG FS may be located away from the normal state FS. We therefore need the quasiparticle excitation energy in the whole BZ to characterize the gap structure. Several typical results are shown in Fig.1 where the minimal quasiparticle excitation energy as a function of momentum in (a) the normal state, (b) a full-gap SC state No.1, (c) a nodal-gap SC state No.5 and (d) a gapless SC state No.11. Here thick white lines (symbols) highlight the zero excitation energy contour (nodal points). By checking the excitation spectra of all possible cases in Tab.I, we summarize that: (i) All $\tau_{1,3}$ -bases are nodal, consistent with the fact that these τ matrices carry $B_{2g,1g}$ representations. (ii) All τ_2 -bases (which carries odd orbital-parity) are gapless (unless the pairing energy scale is of the order of the band width). (iii) The τ_0 -bases leads to full or nodal gaps, depending on the momentum basis function.

Volovik effect and superfluid density In this section, we discuss the physical properties of various SC states, especially the DOS, Volovik effect and superfluid density. We did the calculations for all SC states listed in Tab.I. Since we found that the qualitative behavior is the same for SC states belong to the same category (full-gap, nodal-gap or gapless), we only present the results for representative states, namely, the full-gap SC state No.1, the nodal-gap SC state No.5 and gapless SC state No.11. Fig.2(a) shows the DOS. The low energy U-shaped (V-shaped) DOS in the full-gap (nodal-gap) SC states are conventional. The gapless case is rather exotic. The low energy DOS is not gapped but slightly piled up by SC order,

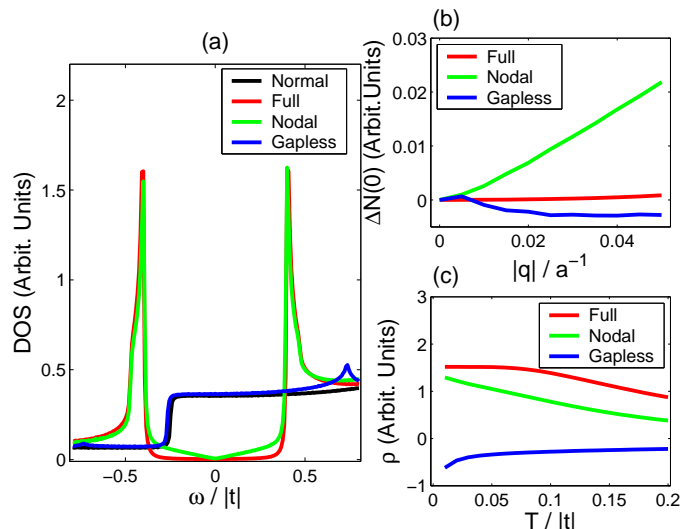


FIG. 2: (Color) Physical properties of various SC states: (a) Density of states; (b) Change of zero energy DOS by a magnetic field $H \propto q^2$; and (c) Low temperature superfluid density.

due to the presence of BdG FS. Fig.2(b) shows the effect of a magnetic field on the DOS, which is calculated by a semi-classical method as follows.[14] The effect of vortices is simulated by averaging over the direction of the superflow momentum \mathbf{q} with $q \propto \sqrt{H}$. The change in zero energy DOS $\Delta N(0, q) = \langle N(0, \mathbf{q}) \rangle - N(0, 0)$ can be probed by the magnetic field dependent specific heat.[4] It is seen in Fig.2(b) that the Volovik effect is absent in the full-gap SC state, but is manifest as a linear rise of ΔN with q in the nodal-gap SC state. Moreover, for the gapless state, the presence of magnetic field actually reduces the DOS (as seen for moderate q). Fig.2(c) shows the temperature dependence of superfluid density. In the low temperature limit we neglect the temperature dependence of the pairing amplitude. The full-gap and nodal-gap SC states exhibit activated and linear drop, respectively. Contrarily, the superfluid density is negative at all temperatures in the gapless case. This arises from the fact that piling up of low energy DOS leads to an overwhelming paramagnetic contribution against the diamagnetic part. It indicates that the gapless state is unstable upon phase twisting, implying a tendency toward possible Fulde-Ferrell-Larkin-Ovchinnikov state or magnetic ordering.

Discussion Basing upon our analysis presented above and recent experiments, we could discuss the possible pairing symmetry of iron-based superconductors. Specific heat[4], NMR[5] penetrate length[7] and tunneling [6] measurements are consistent with spin-singlet nodal pairing with sign changes. On the other hand, on-site singlet pairing is unfavorable to Hund's rule coupling, while bond-wise triplet pairing is inconsistent with the

antiferromagnetic exchange.[15] We are then left with the bond-wise singlet pairing cases No.3,4,6,7,and 9 in Tab.I. Out of these cases we observe that only the A_{2g} case No.4 and the B_{2g} case No.9 have nodal points in the x - and y -directions, which are more relevant if the electron pockets are important. We propose that Raman scattering and phase-sensitive probes could further reduce the redundancy.

Some remarks are in order before closing. First, it should be emphasized that the symmetry classification is robust, while the assignment of a particular pairing symmetry has to be sharpened or even altered according to further systematic and intrinsic experimental results. Second, a general pairing matrix can be decomposed into a linear combination of the bases. In principle, bases belonging to different irreducible representations do not mix, but mixing in other cases can not be ruled out on symmetry ground alone. In particular, the two-dimensional representations, like the case No.10 may be mixed into one of the chiral-symmetry-breaking states shown in No.10'. Third, even if the effect of As ions neglected so far are reconsidered, the point group is still D_{4h} , so that the above symmetry classification still holds. Finally, several authors propose models including d_{xy} or even all five d-orbitals.[16] These may be included in our analysis and result in more pairing bases. For example xy can pair with yz , which transform as x , forming one component of the E representations.

We became aware of a related work[17] after we finished the present paper.

Acknowledgements We thank Feng Zhou for technical help in computation, and Zheng-Yu Weng for helpful discussions. QH thanks The Center of Advanced Study of Tsinghua University where the paper was finalized. The work was supported by NSFC 10325416, the Ministry of Science and Technology of China (under the Grant No. 2006CB921802 and 2006CB601002) and the 111 Project (under the Grant No. B07026).

- [1] Yoichi Kamihara *et al.*, J. Am. Chem. Soc **130**, 3296 (2008); Z. Li *et al.*, Arxiv: 0803.2572; X. H. Chen, *et al.*, Arxiv: 0803.3603; G. F. Chen *et al.*, Arxiv: 0803.3790; H. H. Wen *et al.*, Arxiv: 0804.0835; L. Fang *et al.*, Arxiv: 0803.3978; Z. A. Ren *et al.*, Arxiv: 0803.4283; G. F. Chen *et al.*, Arxiv: 0803.4384; Z. A. Ren *et al.*, Arxiv: 0804.2053; Jie Yang *et al.*, Arxiv: 0804.3727.
- [2] Z. A. Ren *et al.*, Arxiv: 0804.2582.
- [3] H. H. Wen *et al.*, Europhys. Lett **82**,17009(2008).
- [4] Gang Mu *et al.*, Arxiv: 0803.0928.
- [5] Yusuke Nakai *et al.*, Arxiv: 0804.4765.
- [6] Lei Shan *et al.*, Arxiv: 0803.2405.
- [7] S. Luetkens *et al.*, Arxiv: 0804.3115; K. Ahilan *et al.*, Arxiv: 0804.4026.
- [8] K. Haule, J. H. Shim and G. Kotliar, Arxiv: 0803.1279; I. A. Nekrasov Z. V. Pchelkina and M. V. Sadovskii, Arxiv: 0804.1239; A. O. Shorikov *et al.*, Arxiv: 0804.3283; Gang Xu *et al.*, Arxiv: 0803.1282.
- [9] Hai-Jun Zhang *et al.*, Arxiv: 0803.4487; Tao Li, Arxiv: 0804.0536.
- [10] Xi Dai *et al.*, Arxiv: 0803.3982; Qiang Han, Yan Chen and Z. D. Wang, Arxiv: 0803.4346; G. Baskaran, Arxiv: 0804.1341; Zheng-Yu Weng, Arxiv: 0804.3228; Qimiao Si and Elihu Abrahams, Arxiv: 0804.2480; Zi-Jian Yao Jian-Xin Li and Z. D. Wang, Arxiv: 0804.4166; Xiao-Liang Qi *et al.*, Arxiv: 0804.4332; Maria Daghofer, *et al.*, Arxiv: 0805.0148.
- [11] H. Eschrig, Arxiv: 0804.0186.
- [12] E. Volovik and L. P. Gor'kov, JETP Lett. **39**, 674 (1984); Sov. Phys. JETP **61**, 843 (1985); For a review, see, e.g., M. Sigrist and K. Ueda, Rev. Mod. Phys **63**, 239(1991).
- [13] S. Raghu *et al.*, Arxiv: 0804.1113.
- [14] G. E. Volovik, Sov. Phys. JETP **58**, 469(1993).
- [15] G. Giovannetti, S. Kumar and J. van den Brink, Arxiv: 0804.0866; Fengjie Ma and Zhong-Yi Lu, Arxiv: 0804.3286; Fengjie Ma, Zhong-Yi Lu and Tao Xiang, Arxiv: 0804.3370; T. Yildirim, Arxiv: 0804.2252; Z. P. Yin *et al.*, Arxiv: 0804.3355; Fang Chen *et al.*, Arxiv: 0804.3843; Cenke Xu, M Müller and S. Sachdev, Arxiv: 0804.4293.
- [16] Chao Cao, P. J. Hirschfeld and Hai-Ping Cheng, Arxiv: 0803.3236; Kazuhiko Kuroki *et al.*, Arxiv: 0803.3325; Patrick A. Lee and Xiao-Gang Wen, Arxiv: 0804.1739. V. Cvetkovic and Z. Tesanovic, Arxiv: 0804.4678.
- [17] Zhi-Hui Wang *et al.*, Arxiv: 0805.0736.

* E-mail address:qhwang@nju.edu.cn